energies

MDPI

Article

A Controller for Optimum Electrical Power Extraction from a Small Grid-Interconnected Wind Turbine

Tania García-Sánchez [1,†], Arbinda Kumar Mishra [2,†], Elías Hurtado-Pérez [1,†], Rubén Puché-Panadero [1,†] and Ana Fernández-Guillamón [3,*,†]

1 Department of Electrical Engineering, Universitat Politècnica de València, 46022 Valencia, Spain; tagarsan@die.upv.es (T.G.-S.); ejhurtado@die.upv.es (E.H.-P.); rupucpa@die.upv.es (R.P.-P.)
2 Department of Electrical Engineering, Pulchowk Campus, Institute of Engineering, Tribhuvan University, Dharan 56700, Nepal; akmishra@ioe.edu.np
3 Department of Automatics, Electrical Eng. and Electronic Tech., Universidad Politécnica de Cartagena, 30202 Cartagena, Spain
* Correspondence: ana.fernandez@upct.es; Tel.: +34-968-325357
† These authors contributed equally to this work.

Received: 10 September 2020; Accepted: 4 November 2020; Published: 6 November 2020

Abstract: Currently, wind power is the fastest-growing means of electricity generation in the world. To obtain the maximum efficiency from the wind energy conversion system, it is important that the control strategy design is carried out in the best possible way. In fact, besides regulating the frequency and output voltage of the electrical signal, these strategies should also extract energy from wind power at the maximum level of efficiency. With advances in micro-controllers and electronic components, the design and implementation of efficient controllers are steadily improving. This paper presents a maximum power point tracking controller scheme for a small wind energy conversion system with a variable speed permanent magnet synchronous generator. With the controller, the system extracts optimum possible power from the wind speed reaching the wind turbine and feeds it to the grid at constant voltage and frequency based on the AC–DC–AC conversion system. A MATLAB/SimPowerSystems environment was used to carry out the simulations of the system. Simulation results were analyzed under variable wind speed and load conditions, exhibiting the performance of the proposed controller. It was observed that the controllers can extract maximum power and regulate the voltage and frequency under such variable conditions. Extensive results are included in the paper.

Keywords: small wind; maximum power point tracking; type 4; variable speed wind turbine; wind turbine control

1. Introduction

Nowadays, most countries are promoting the massive integration of renewable energy sources (RES) to replace conventional power plants based on nuclear and fossil fuels [1,2]. Among the different reasons for this transition, the most important include the environmental worry (climate change due to greenhouse gas emissions) and also to reduce the energy dependence on fuels imported from third countries [3,4]. However, RES have a stochastic and uncertain behavior due to their dependence on weather conditions [5]. Indeed, this is considered as an important drawback for their massive integration, as they impose stress on the power systems' operation [6,7]. Among the different RES available, wind energy is widely considered as the most economic, qualified and inexhaustible resource [8,9]. In fact, the cumulative installed wind

capacity has increased non-stop since 2001, currently accounting for more than 650 GW worldwide [10]. Moreover, another important strength of wind turbines is that their applications vary in accordance to their size [11]. Consequently, apart from the huge wind power plants, small wind installations have greatly increased in remote areas with a complex terrain, being considered as a cost-effective solution for areas which are not connected to the main grid, or where the grid power availability is insufficient [12,13]. In fact, there are currently more than 250 small wind turbine manufacturers, and the number of installations is more than one million worldwide [14].

Wind turbines can be classified into: (i) fixed speed wind turbines (FSWTs) and (ii) variable speed wind turbines (VSWTs) [15]. FSWTs are equipped with induction generators (squirrel cage or wound rotor), thereby being simpler and requiring lower construction and maintenance costs. However, their operation rotational speed is fixed and cannot be controlled if wind speed varies from one value to another. In contrast, VSWTs use doubly-fed induction generators (DFIG) or permanent magnet synchronous generators (PMSG) with a partial or full-scale converter, respectively. Due to this power electronic converter, VSWTs can adjust their rotor speed according to the wind speed, extracting the maximum mechanical power from the wind speed [16]. Therefore, their efficiency is higher than the efficiency of FSWTs; thus, they are preferred over FSWTs [17,18]. Nowadays, PMSG are becoming more popular due to their reliability, gear-less configuration and light weight [19,20]. Indeed, for small wind energy applications, PMSG are becoming an attractive option for distributed generation due to their efficiency and system simplicity [21–23].

The optimum power extraction control (also known as maximum power point tracking, MPPT) is in charge of extracting the maximum mechanical power from the wind, thereby playing a key role in increasing the efficiency (maximizing the energy production) of the wind conversion system [24,25]. Even though large wind turbines combine a turbine control (pitch-angle control) and a generator control, small wind turbines do not usually include pitch controllers [26]. In this way, the complexity of the turbine and the cost of the system are lower [27]. Furthermore, due to the reduced height of small wind turbines, wind finds more obstacles (trees, buildings, hillsides, etc.), and it becomes more turbulent [28]. Consequently, several studies have focused on the MPPT technique for small wind turbines. Jeong et al. proved the capability of a combined method of hysteresis control with tip speed ratio (TSR) control, by using both simulations and experiments [29]. The theory of power feedback and hill climb searching was used in [30] for a novel optimal current given the MPPT control strategy. Chen and Hung proposed a systematic experimental verification of chaos-embedded sliding mode extremum in order to determine the MPPT control, thereby obtaining better dynamic results than traditional control schemes [31]. An MPPT control based on the extended perturb and observe method was proposed in [32], proving that the proposed methodology increased the efficiency of the small wind turbine system. Recently, different sensor-less algorithms have also been presented [33–35].

This paper proposes an optimum control system for a small wind turbine to regulate the output power from a wind energy conversion system connected to a grid. Following the MPPT control methods for PMSG presented in [36], a tip speed ratio control is used in this optimum control system, in which the maximum power points are tracked, and by choosing the optimum tip speed ratio, the optimum speed reference is obtained. A VSWT with a PMSG and a full-scale converter was used as case study. The novelty of the proposed controller is based on its simplicity, as only the equations of the PMSG are required. The MPPT control algorithm has been introduced to regulate the rotational speed to force the PMSG to work around its maximum power point. The PWM IGBT/diode-based generator and side converter controllers control the rotor speed and torque with PI controllers. This optimizes the power extraction from the wind at variable wind speed. The rest of the paper is organized as follows: Section 2 presents the main equations and parameters of a wind turbine, together with the characteristics and particularities of small wind and the electrical equations of the PMSG in the dq-frame; the control strategy for optimum

electrical power extraction proposed in the paper is described in Section 3; Section 4 analyzes the results; finally, Section 5 gives the conclusions of the study.

2. Wind Turbine Generalities: Small Wind and PMSG

The turbine blades catch the wind and convert it into mechanical energy. As the hub of the rotor is connected to the electrical generator though the shaft, that rotational mechanical energy is converted into electricity. The relationship between the wind speed (s_w) and the aerodynamic available wind power (P_w) can be expressed by Equation (1):

$$P_w = \frac{1}{2} \cdot \rho \cdot A \cdot {s_w}^3 , \tag{1}$$

where ρ is the air density and A is the swept area by the blades.

The mechanical power (P_{mech}) extracted by the wind turbine is only a fraction of the available power. Indeed, the power coefficient (C_p) measures the efficiency of the first conversation from wind speed to mechanical power. This coefficient depends on the wind speed and the rotor speed, with a maximum value of 59.3% according to the Betz limit [37]. The extracted mechanical power is then given by Equation (2):

$$P_{mech} = C_P(\beta, \lambda) \cdot P_w . \tag{2}$$

Thus, the power coefficient can be understood as the aerodynamic efficiency of the rotor. It depends on the blade pitch angle (β) and the tip speed ratio (λ). The tip speed ratio (λ) is defined as the ratio between the peripheral speed of the blades ($\Omega \cdot R$ and the wind speed, following Equation (3):

$$\lambda = \frac{\Omega \cdot R}{s_w} , \tag{3}$$

where Ω is the rotor speed of the turbine and R is the rotor radius. In the particular case of small wind turbines, they do not usually include a gearbox. Consequently, the rotor speed and the generator speed are the same ($\Omega = \omega$). Moreover, the pitch-angle is normally considered as fixed, as already mentioned in Section 1. Hence, for small wind, the power coefficient only depends on λ, as depicted in Figure 1.

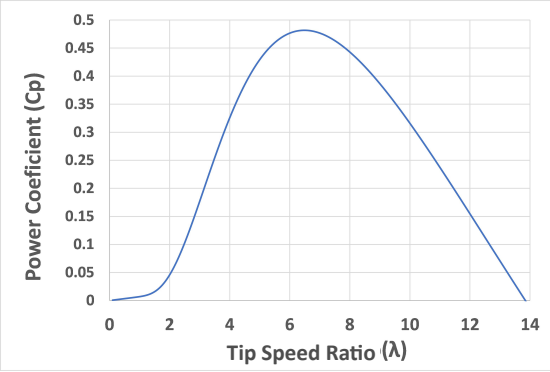

Figure 1. Power coefficient vs. tip speed ratio curve.

The maximum power P_{MPP} is extracted from the wind speed when the wind turbine operates at the maximum power coefficient $C_{p,max}$. For a typical wind turbine with a power coefficient characteristic like the one shown in Figure 1, the extracted power versus the tip speed ratio is depicted in Figure 2. It can be seen that the aerodynamic efficiency of a wind turbine is maximal for a specific value of tip speed ratio. Hence, by keeping the tip speed ratio at its optimum value (λ_{opt}) through the rotor speed, the maximum

power at available wind speed P_{MPP} can be extracted. Consequently, if the wind speed changes, the rotor speed should be adjusted to follow said variation.

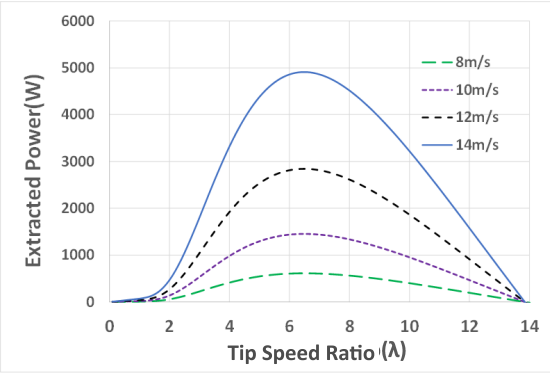

Figure 2. Extracted power P_m vs. tip speed ratio Λ at varying wind speed.

2.1. Small Wind

Different definitions are found in the specific literature when referring to small wind turbines: for instance, Urtasun et al. considers that small wind turbines refer to those wind turbines of up to 100 kW [38]. A more concise definition is provided in [39], where it is specified that small wind turbines only include wind turbines with a swept area by the rotor $A < 200$ m^2, and powers between 1–15 kW for residential purposes or 15–100 kW for light commercial installations. On the other hand, Muhsen et al. refers to small wind turbines as those with rated power of less than 50 kW [40]. In any case, it is generally agreed that small wind installations are convenient for isolated areas, which are difficult to connect to the main grid due to technical and/or economical limitations [41].

Nowadays, electricity is a key element to developing the economy of any region. However, almost 17% of the world's population does not have access to it, and most of them (nearly 90%) live in rural areas of poor tropical regions [42,43]. Small wind installations only require small foundation plots, with a short construction time (a few months). Moreover, if electricity is generated and consumed in neighborhood areas, these small installations substantially reduce the investment needed to generate and distribute electricity from centralized power plants, also minimizing the losses due to long distance transmissions. Consequently, small wind systems can play an important and practical role in generating reliable and affordable electricity for poor rural areas, reducing their poverty [44].

Together with this, there are also different applications for small wind turbines, such as lifting water to tanks located high, or pumping it from underground [45]; integrating small wind turbines into buildings, or installing them on the rooftops, especially on high-rise buildings [46]; and even providing electricity to on-grid consumers which will supply its excess to the power system (which are usually referred to as prosumers) [47,48].

As small wind installations are commonly located where the electricity is required, these areas can have poor wind conditions [49]. In fact, when they operate in urban zones, they are exposed to severe wind gusts, with fast fluctuations and turbulent winds, which can affect the performance of the wind turbine [50]. These characteristics are due to the following three reasons: (i) the interaction between the wind and the building structures; (ii) the high surface roughness; and (iii) the atmospheric instabilities due to local heat sources [51]. Consequently, due to the influence of wind speed changes on the wind turbine performance, direct driven PMSG are considered as the best alternative for small wind applications, as the permanent magnets produce the magnetic flux without needing any additional element for excitation [52].

2.2. Permanent Magnet Synchronous Generator

From the 650 GW of wind power installed worldwide, 35% corresponds to VSWTs equipped with a full-scale converter and PMSG [53]. To model a synchronous machine of a PMSG, projection of phase quantities in a rotating dq-axis greatly simplifies the model, as time varying parameters are simplified to a time independent parameters [54,55]. In the rotating reference frame, the dynamic equations representing the behavior of a PMSG are expressed in Equations (4) and (5) [56]:

$$V_d = -R_s \cdot I_d - L_d \cdot \frac{dI_d}{dt} + \omega \cdot L_q \cdot I_q \,, \tag{4}$$

$$V_q = -R_s \cdot I_q - L_q \cdot \frac{dI_q}{dt} - \omega \cdot L_d \cdot I_d + \omega \cdot \phi_m \,, \tag{5}$$

where V_d and V_q are the d-axis and q-axis components of the voltage, R_s is stator winding resistance, L_d and L_q are d-axis and q-axis inductances, ω is the generator speed, I_d and I_q are the d-axis and q-axis components of the current and ϕ_m is PMSG magnetic flux. The electromagnetic torque of the rotor can be expressed as Equation (6), p being the number of poles:

$$T_e = \frac{3}{2}\left(\frac{p}{2}\left[(L_d - L_q) \cdot I_d \cdot I_q + \phi_m \cdot I_q\right]\right) . \tag{6}$$

The PMSG type is considered as a surface mounted magnet; therefore, L_d and L_q are almost equal ($L_d \approx L_q$) [56]. Consequently, the electromagnetic torque in the rotor simplifies to Equation (7):

$$T_e = \frac{3 \cdot p}{4} \cdot \phi_m \cdot I_q \,. \tag{7}$$

Moreover, the wind turbine torque and electromagnetic torque are related through the so-called swing-equation (8):

$$T_m - T_e = J \cdot \frac{d\omega}{dt} + D \cdot \omega \,, \tag{8}$$

where the inertia J and damping friction coefficient D are combined for both turbine and generator.

3. Optimum Electrical Power Extraction

For a VSWT with a PMSG and a back-to-back full-scale converter, it is possible to control both the rotor speed and generated electromagnetic torque. This way, the tip speed ratio can be maintained at the optimum value so that the aerodynamic efficiency is at its maximum ($C_{p,max}$), which means that the energy conversion is maximized.

The basic control philosophy comes from Equations (7) and (8) of Section 2. As already described, the extracted mechanical power does not only depend on the wind speed, but also on the rotor speed (refer to Equation (2) in Section 2). By correlating the PMSG electromagnetic torque with the rotor speed using Equation (8), and taking the Laplace transform, Equation (9) is gotten:

$$\frac{\omega(s)}{T_m(s) - T_e(s)} = \frac{1}{Js + D} \,. \tag{9}$$

Similarly, Equation (7) can be expressed as:

$$T_e(s) = K \cdot I_q(s) \,, \tag{10}$$

where K is a constant obtained as:

$$K = \frac{3 \cdot p}{4} \cdot \phi_m \,. \tag{11}$$

Equations (9) and (10) can be represented in a mathematical block diagram, as shown in Figure 3. This diagram is the speed control block diagram of a PMSG. In order to control the rotor speed to a specified (reference) value, the required reference current $I_{q,ref}$ can be obtained as indicated in the diagram. According to Equation (8), and as was presented in Sections 1 and 2, small wind turbines with PMSG do not usually include a gearbox. Consequently, the speeds of the PMSG (ω) and of the blades (Ω) are the same, and a one-mass mechanical model (mathematically expressed in terms of Equation (8)) is enough to determine such a rotational speed. Following this, and with the block diagram of Figure 3, only ω_{ref}, PI values, K, J, D and T_m are needed to obtain the rotational speed:

- ω_{ref} is estimated from the wind speed s_w and considering Equation (3). As the aim is to obtain the optimum value of λ (λ_{opt}), and according to the specific literature, its optimum value is between 6.5 and 7.5 [57], the reference value of $\omega = \Omega$ is obtained by choosing a λ value within that range.
- PI values are presented in Table 1.
- K is determined following Equation (11), where p and ϕ_m are given in Table 1.
- J and D are given in Table 1.
- T_m is determined from $T_m = P_{mech}/\Omega$, using the mechanical power (Equation (2)) and the rotational speed $\Omega = \omega$.

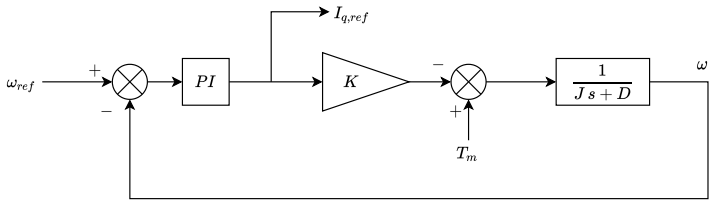

Figure 3. Mathematical block-diagram for I_q and ω.

Since the electromagnetic torque is directly proportional only to the q-axis current I_q, for the same electromagnetic torque, the generator voltage drop and power losses can be minimized by setting the d-axis current to zero, $I_d = 0$. The two reference currents ($I_{q,ref}$ obtained above and $I_{d,ref}$ set to zero) can then be used to determine the reference dq-axis voltages for the generator using Equations (4) and (5) from Section 2. This is depicted in the mathematical block diagram representation in Figure 4.

The tuning of the PI controllers for the speed controller in Figure 3 depends on the combined inertia and damping friction coefficients of turbine and PMSG rotor, whereas the tuning of the PI current controllers of Figure 4 depends on the stator winding resistance and inductance of PMSG. Hence, these controllers' parameters are independent of the wind speed. In operating conditions, signals I_d, I_q and ω are feedback signals from the generator. The V_d and V_q references obtained from the block diagram of Figure 4 are then used to generate the gate signal sequences for the six IGBTs of the generator side converter after converting these to the phase quantities and normalizing them with the DC output voltage of the converter.

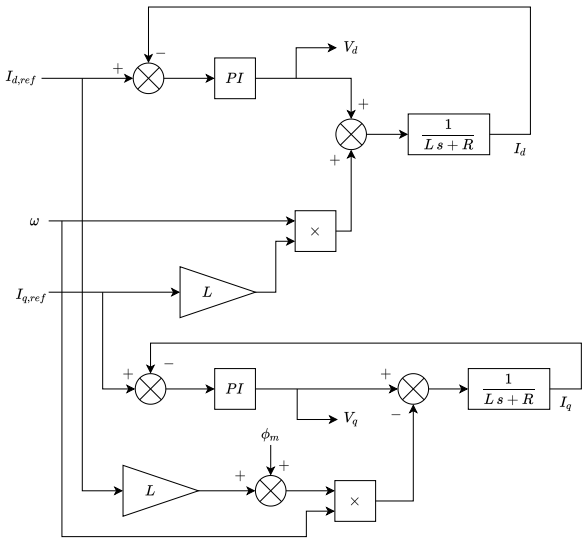

Figure 4. Mathematical block-diagram for V_d and V_q reference generation with current decoupling.

Table 1. Parameters for simulation.

Parameter	Symbol	Value	Controller	Value
PMSG stator resistance	R_s	0.425 Ω	$K_{p,\omega}$	70
PMSG inductance	$L_d = L_q$	8.4 mH	$K_{i,\omega}$	960
Generator poles	p	8	K_{p,i_d}	20
Flux linkage of PMSG	ϕ_m	0.433 Wb·t	K_{i,i_d}	720
Wind turbine blade radius	R	1.75 m	K_{p,i_q}	20
Combined inertia of rotor	J	0.02 kg m^2	K_{i,i_q}	720
Friction factor	D	0.0002 N m s		

4. Results

The wind turbine model is based on the Anelion SW 3.5 GT wind turbine [58]. The power curve of the wind turbine under consideration is presented in Figure 5: the black line is the power curve according to IEC 61400-12, whereas orange and gray lines depict the maximum and minimum operation range, respectively. The generator rectifier is responsible for the rotor speed control [59]. This controller optimizes the power extraction from the wind at variable wind speed. This is achieved by a control system that generates the appropriate sequences of gate signals for the converter IGBTs. The grid-side inverter is simply a current source inverter feeding the extracted electrical power instantly to the grid at constant voltage and frequency.

Figure 6 represents the small wind turbine system connected to a grid. This includes the wind turbine and PMSG, the generator side and grid-side converters, an electrical line and the AC grid. The wind energy conversion system depicted in Figure 6 was implemented in detail using the MATLAB/SimPowerSystems environment, in line with several published papers [60–63]. SimPowerSystems is a MATLAB tool to model and simulate electric power systems in the Simulink environment, allowing users to perform different studies (such as power flow analysis, frequency analysis and transient analysis) [64]. In this case, authors analyzed the performance of the proposed optimum electrical power extraction model under wind speed variations and load variations. The generator and turbine parameters considered for this study are presented in Table 1.

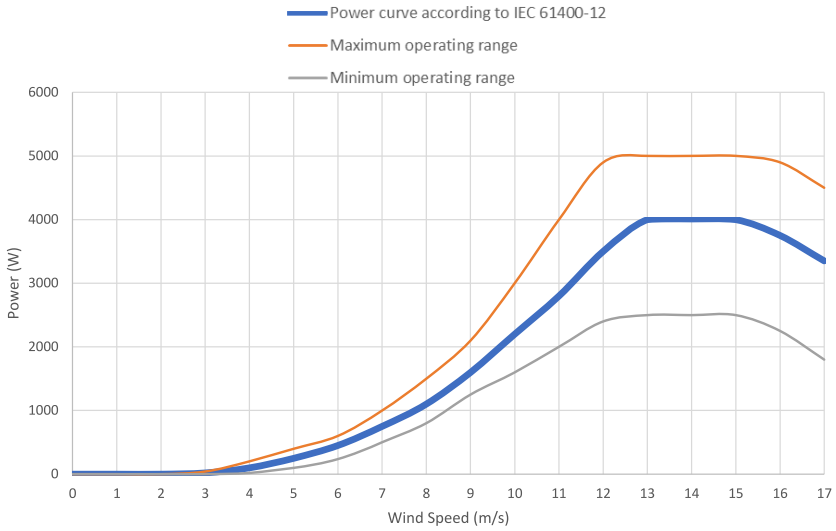

Figure 5. Power curve of the Anelion SW 3.5 GT wind turbine.

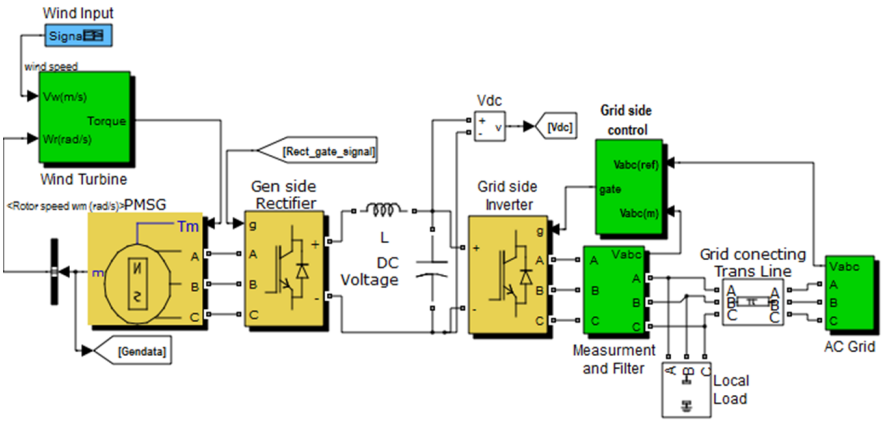

Figure 6. Small wind energy conversion system.

4.1. Wind Speed Variation

Figure 7 presents the main results from the simulation with variable wind speed. The initial wind speed was fixed at 10 m/s; then, at 1.1 s, the speed dropped to 8 m/s, and at 1.6 s, the speed raised to 9 m/s (Figure 7a). In this way, it is possible to analyze the behavior of the small wind turbine, both when wind speed decreases and when it increases. As can be seen from the power coefficient C_p depicted in Figure 7b, it only suffers from small transients in the time-moment when the wind speed changes (at $t = 1.1$ s and $t = 1.6$ s). For the rest of the time under analysis, it is maintained as constant at nearly its maximum value, ensuring that the controller is able to maintain a constant top speed ratio under the varying wind speed. The rotor speed simultaneously and proportionally changes with the wind speed, both the reference (black line) and the actual (pink line) rotor speeds. Moreover, the actual rotor speed faithfully follows the reference one for optimum system operation under increasing and decreasing wind speed variations. Due to the mathematical relationship between power, torque and speed ($P = T \cdot \Omega$), the extracted power from the turbine of Figure 7d is in line with the rotor speed of Figure 7c and the turbine torque of Figure 7f (pink line). In fact, as can be seen from Figure 7f, turbine torque only suffers from small transients in the time-moment when the wind speed changes, which last less than 0.01 s. Moreover, and comparing the

results with the power curve of the wind turbine considered, it can be seen that the extracted turbine power shown in Figure 7d represents the maximum power (refer to Figure 5).

The current control characteristic (Figure 7e) clearly indicates that the q-axis current I_q (black line) is changing in line with the wind speed. Since the electromagnetic torque generated by the PMSG (black line of Figure 7f) changes proportionally with this q-axis current, this results in an optimum extraction of the wind turbine power, as depicted in Figure 7d. In fact, the d-axis PMSG current I_d (pink line of Figure 7e) is maintained to a zero value except for some small transients when the wind speed changes. In this way, the generator voltage drop and power losses are minimized, as already justified in Section 3.

The inverter outputs are shown in Figure 7g–i in terms of AC output voltage, AC output current and 3-phase power. These are the AC grid-side characteristics of the system. As can be seen, the voltage remained constant during the whole simulated time-period, equal to 1 p.u. In contrast, the three phase inverter AC current changes with the wind speed variations, firstly reducing from 2.5 A to 1.95 A, and then increasing to 2.1 A. Due to the relationship between active power, voltage and current ($P = V \cdot I$), the output power of the small wind turbine system changes due to the dependence of current and wind speed; subsequently, the output power also changes in line with the wind speed.

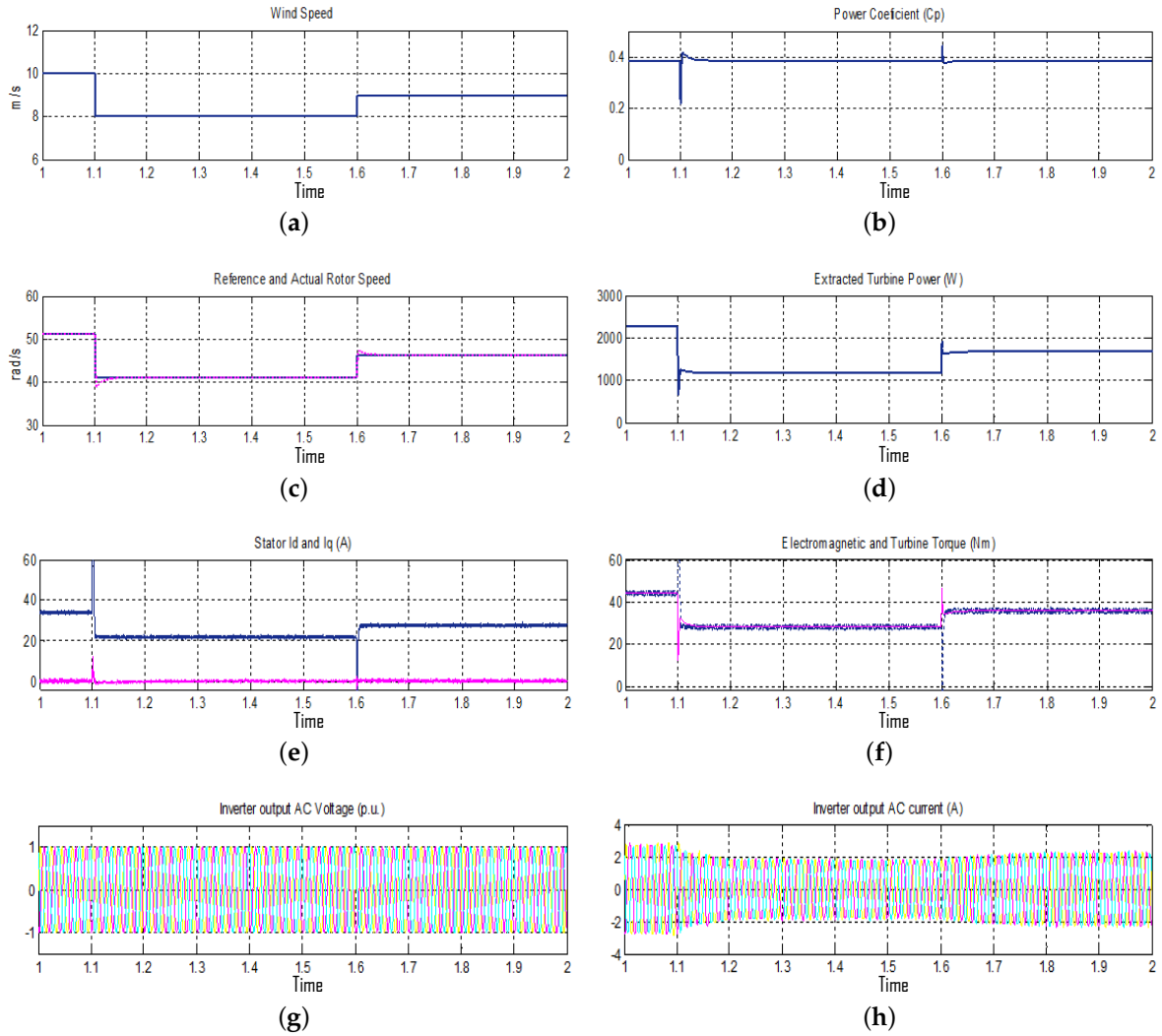

Figure 7. *Cont.*

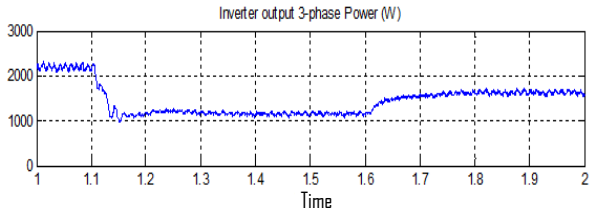

(**i**)

Figure 7. Results for variable wind speed. (**a**) Wind speed. (**b**) Power coefficient. (**c**) Rotor speed. (**d**) Turbine power. (**e**) Stator currents. (**f**) Torques. (**g**) Inverter AC voltage. (**h**) Inverter AC current. (**i**) Inverter power.

4.2. Local Load Variation

Figure 8 presents the main results from the simulation with variable load. Initially, a load of 2 kW was connected immediately after the inverter (in between the inverter and the grid), as marked in Figure 6. Two more loads, each one of them of 2 kW, were then added at 0.6 s and 1 s, respectively. In this case, the wind speed was kept constant at 11 m/s, as shown in Figure 8a. Due to the constant wind speed, both the power coefficient and the rotor speed were maintained at their optimum values for such wind speed value (refer to Figure 8b,c). Additionally, the extracted turbine power (Figure 8d), stator currents (Figure 8e), and torques (Figure 8f) were kept constant under constant wind speed. Consequently, under constant wind speed with variable local load, no torque peaks were obtained. Hence, we witnessed that the system was operating at its optimum point without any disturbances on the generator side performance of the system.

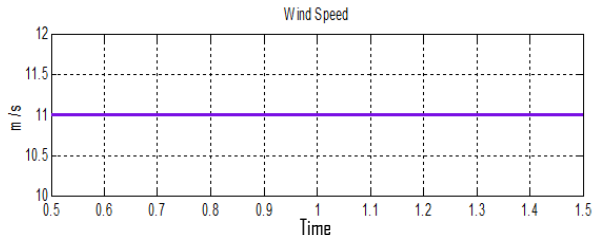

(**a**)

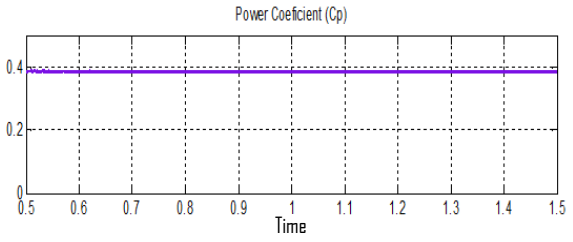

(**b**)

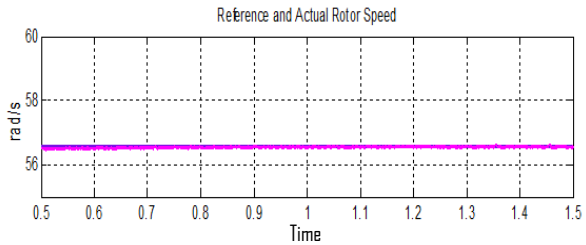

(**c**)

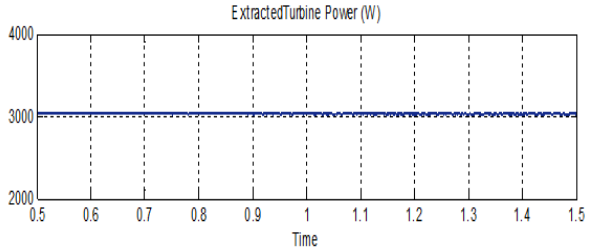

(**d**)

Figure 8. *Cont.*

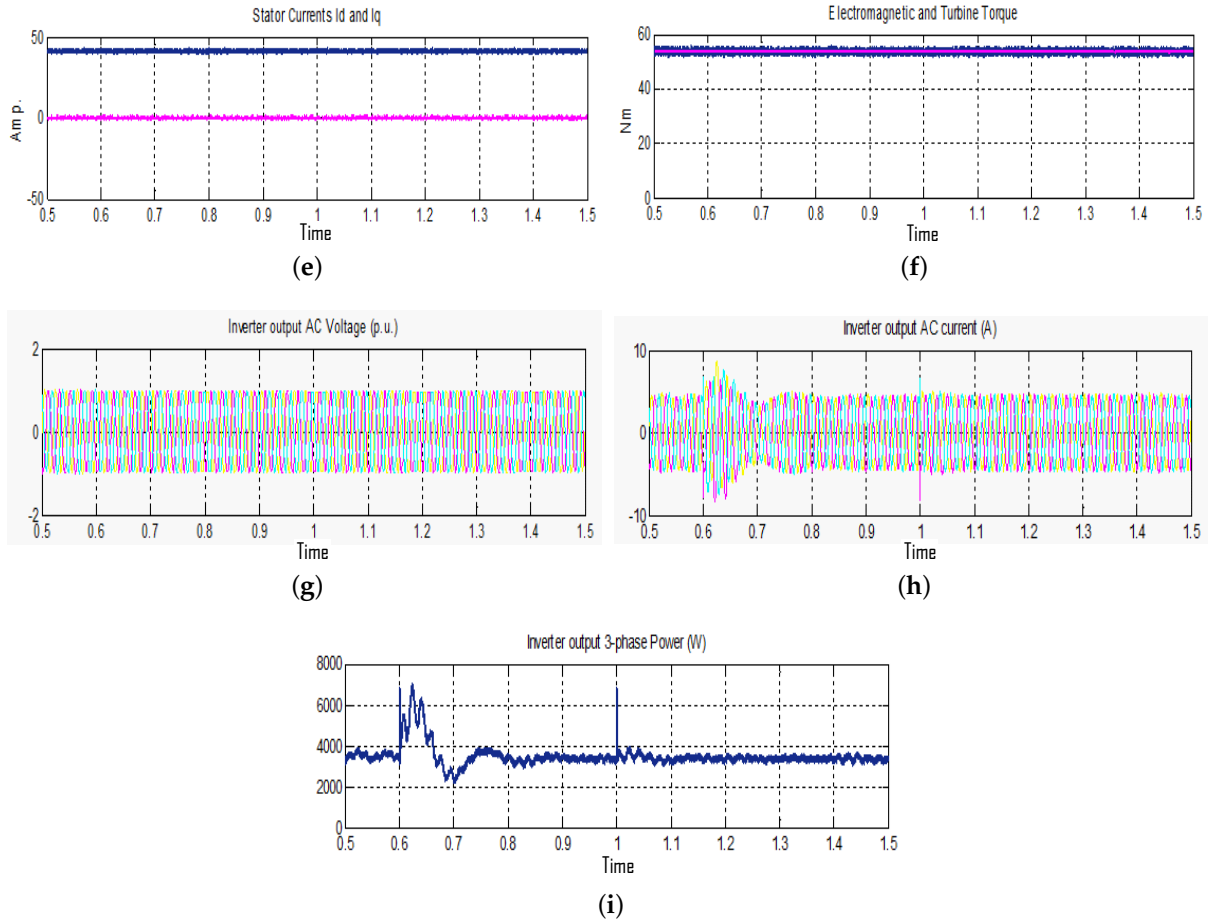

Figure 8. Results for variable load. (**a**) Wind speed. (**b**) Power coefficient. (**c**) Rotor speed. (**d**) Torques. (**e**) Turbine power. (**f**) Stator currents. (**g**) Inverter AC voltage. (**h**) Inverter AC current. (**i**) Inverter power.

With regard to the inverter output of Figure 8g–i, voltage was again maintained at 1 pu. However, some transients were found for the current and power output values when the load increased. Consequently, this means that in steady state, there is no effect even in the inverter output for local load variation. In fact, it is interesting that even though the new added loads had the same power (2 kW each), the transient of the first load at $t = 0.6$ s was bigger and longer than the one at $t = 1$ s. This is because before the first load was added ($t < 0.6$ s), the power was flowing from system to the initial load and the grid. Then, when the first load was added at $t = 0.6$ s, the power flow changed its direction (from grid towards the new loads) to fulfill the new consumed power. Consequently, at $t = 0.6$ s, there was a sudden transition of the power flow to/from the grid. However, when the second load was included at $t = 1$ s, the direction of the power flow from the grid remained unchanged even with the change in local demand.

5. Conclusions

This paper has presented a maximum power point tracking controller scheme for a grid-interconnected variable speed small wind turbine with a PMSG. The controllers generated the appropriate gate signal sequence for PWM generator side converter to control the rotor speed and torque with PI controllers. It has been observed that with the controller, the rotor speed simultaneously and

proportionally changes with the wind speed. The power coefficient was maintained constant nearly to its maximum value except small transients at the instant of wind speed change. This ensures the optimum possible power extraction from the wind turbine with varying wind speed. Only short-time transients were obtained when the wind speed changed, thereby implying less stress from the wind turbine point of view. It was also witnessed that the system was operating tat its optimum with no disturbances on the generator side performance of the system with variation in load. However, if the change of load caused the reversal of power flow direction to and from the grid, some major transients were observed in the inverter output currents and power. The tuning of the PI controllers only depends on the inertia and damping friction coefficients of the turbine generator rotor and stator winding resistance, and the inductance of the generator, without any dependency on the wind speed.

Author Contributions: Conceptualization, A.K.M. and A.F.-G.; methodology, A.K.M. and T.G.-S.; software, T.G.-S.; validation, T.G.-S., A.K.M., E.H.-P. and R.P.-P.; formal analysis, A.F.G.; investigation, T.G.-S.; resources, T.G.-S. and A.K.M.; data curation, A.F.G.; writing—original draft preparation, T.G.-S. and A.K.M.; writing—review and editing, A.F.-G.; visualization, A.F.-G.; supervision, E.H.-P. and R.P.-P.; project administration, T.G.-S. and A.F.G.; funding acquisition, A.K.M., E.H.-P. and A.F.-G. All authors have read and agreed to the published version of the manuscript.

Funding: This work was partially supported by the Spanish Ministry of Education, Culture and Sports—reference FPU16/04282.

Conflicts of Interest: The authors declare no conflict of interest.

Abbreviations

The following abbreviations are used in this manuscript:

β	blade pitch angle
λ	tip speed ratio
ρ	air density
ϕ_m	PMSG magnetic flux
ω	generator speed
Ω	rotor speed
p	number of pairs of poles
s_w	wind speed
A	swept area by the blades
C_p	power coefficient
$C_{p,max}$	maximum power coefficient
D	damping friction coefficient
H	inertia constant
I_d	d-axis components of the current
$I_{d,ref}$	reference current
I_q	q-axis components of the current
$I_{q,ref}$	reference current
L_d	d-axis inductance
L_q	q-axis inductance
P_{mech}	mechanical power
P_{mpp}	maximum power
P_w	wind power
R_s	stator winding resistance
T_e	electromagnetic torque
T_m	wind turbine torque
V_d	d-axis components of the voltage
V_q	q-axis components of the voltage
FSWT	Fixed Speed Wind Turbine

MPPT Maximum Power Point Tracking
PMSG Permanent Magnet Synchronous Generator
VSWT Variable Speed Wind Turbine

References

1. Fernández-Guillamón, A.; Villena-Lapaz, J.; Vigueras-Rodríguez, A.; García-Sánchez, T.; Molina-García, Á. An adaptive frequency strategy for variable speed wind turbines: Application to high wind integration into power systems. *Energies* **2018**, *11*, 1436. [CrossRef]
2. Fernández-Guillamón, A.; Sarasúa, J.I.; Chazarra, M.; Vigueras-Rodríguez, A.; Fernández-Muñoz, D.; Molina-García, A. Frequency control analysis based on unit commitment schemes with high wind power integration: A Spanish isolated power system case study. *Int. J. Electr. Power Energy Syst.* **2020**, *121*, 106044. [CrossRef]
3. Huber, M.; Dimkova, D.; Hamacher, T. Integration of wind and solar power in Europe: Assessment of flexibility requirements. *Energy* **2014**, *69*, 236–246. [CrossRef]
4. Fernández-Guillamón, A.; Martínez-Lucas, G.; Molina-García, Á.; Sarasua, J.I. Hybrid Wind–PV Frequency Control Strategy under Variable Weather Conditions in Isolated Power Systems. *Sustainability* **2020**, *12*, 7750. [CrossRef]
5. Fernández-Guillamón, A.; Vigueras-Rodríguez, A.; Molina-García, Á. Analysis of power system inertia estimation in high wind power plant integration scenarios. *IET Renew. Power Gener.* **2019**, *13*, 2807–2816. [CrossRef]
6. Fernández-Guillamón, A.; Das, K.; Cutululis, N.A.; Molina-García, Á. Offshore wind power integration into future power systems: Overview and trends. *J. Mar. Sci. Eng.* **2019**, *7*, 399. [CrossRef]
7. Muñoz-Benavente, I.; Hansen, A.D.; Gómez-Lázaro, E.; García-Sánchez, T.; Fernández-Guillamón, A.; Molina-García, Á. Impact of combined demand-response and wind power plant participation in frequency control for multi-area power systems. *Energies* **2019**, *12*, 1687. [CrossRef]
8. Gil-García, I.C.; García-Cascales, M.S.; Fernández-Guillamón, A.; Molina-García, A. Categorization and analysis of relevant factors for optimal locations in onshore and offshore wind power plants: A taxonomic review. *J. Mar. Sci. Eng.* **2019**, *7*, 391. [CrossRef]
9. Molina-García, A.; Fernández-Guillamón, A.; Gómez-Lázaro, E.; Honrubia-Escribano, A.; Bueso, M.C. Vertical wind profile characterization and identification of patterns based on a shape clustering algorithm. *IEEE Access* **2019**, *7*, 30890–30904. [CrossRef]
10. Global Wind Report 2019. Available online: https://gwec.net/global-wind-report-2019/ (accessed on 15 August 2020).
11. Chagas, C.C.M.; Pereira, M.G.; Rosa, L.P.; da Silva, N.F.; Freitas, M.A.V.; Hunt, J.D. From Megawatts to Kilowatts: A Review of Small Wind Turbine Applications, Lessons From The US to Brazil. *Sustainability* **2020**, *12*, 2760. [CrossRef]
12. Culotta, S.; Franzitta, V.; Milone, D.; Moncada Lo Giudice, G. Small wind technology diffusion in suburban areas of Sicily. *Sustainability* **2015**, *7*, 12693–12708. [CrossRef]
13. Nazir, M.S.; Wang, Y.; Muhammad, B.; Hafiz M, S.; Kadhem, A.A.; Nazir, H.; Abdalla, A.N.; Ma, Y. Comparison of Small-Scale Wind Energy Conversion Systems: Economic Indexes. *Clean Technol.* **2020**, *2*, 144–155. [CrossRef]
14. Polat, A.; Ergene, L.T. A New MPPT Method with Fuzzy Logic Tuning in Small Scale Wind Energy Conversion Systems. In Proceedings of the 2019 11th International Conference on Electrical and Electronics Engineering (ELECO), Bursa, Turkey, 28–30 November 2019; pp. 91–95.
15. García-Sánchez, T.; Muñoz-Benavente, I.; Gómez-Lázaro, E.; Fernández-Guillamón, A. Modelling Types 1 and 2 Wind Turbines Based on IEC 61400-27-1: Transient Response under Voltage Dips. *Energies* **2020**, *13*, 4078. [CrossRef]
16. Fernández-Guillamón, A.; Martínez-Lucas, G.; Molina-García, Á.; Sarasua, J.I. An Adaptive Control Scheme for Variable Speed Wind Turbines Providing Frequency Regulation in Isolated Power Systems with Thermal Generation. *Energies* **2020**, *13*, 3369. [CrossRef]

17. Tiwari, R.; Padmanaban, S.; Neelakandan, R.B. Coordinated control strategies for a permanent magnet synchronous generator based wind energy conversion system. *Energies* **2017**, *10*, 1493. [CrossRef]
18. Sajadi, M.; De Kooning, J.D.; Vandevelde, L.; Crevecoeur, G. Harvesting wind gust energy with small and medium wind turbines using a bidirectional control strategy. *J. Eng.* **2019**, *2019*, 4261–4266. [CrossRef]
19. Pandey, A.K. Performance Analysis of PMSG Wind Turbine at Variable Wind Speed. In Proceedings of the 2018 5th IEEE Uttar Pradesh Section International Conference on Electrical, Electronics and Computer Engineering (UPCON), Gorakhpur, India, 2–4 November 2018; pp. 1–6.
20. Chavero-Navarrete, E.; Trejo-Perea, M.; Jáuregui-Correa, J.C.; Carrillo-Serrano, R.V.; Ríos-Moreno, J.G. Expert control systems for maximum power point tracking in a wind turbine with PMSG: state of the art. *Appl. Sci.* **2019**, *9*, 2469. [CrossRef]
21. Orlando, N.A.; Liserre, M.; Mastromauro, R.A.; Dell'Aquila, A. A survey of control issues in PMSG-based small wind-turbine systems. *IEEE Trans. Ind. Inform.* **2013**, *9*, 1211–1221. [CrossRef]
22. Sokolovs, A.; Grigans, L. Front-end converter choice considerations for PMSG-based micro-wind turbines. In Proceedings of the 2015 56th International Scientific Conference on Power and Electrical Engineering of Riga Technical University (RTUCON), Riga, Latvia, 14 October 2015; pp. 1–6.
23. Daili, Y.; Gaubert, J.P.; Rahmani, L.; Harrag, A. Quantitative feedback theory design of robust MPPT controller for small wind energy conversion systems: design, analysis and experimental study. *Sustain. Energy Technol. Assess.* **2019**, *35*, 308–320. [CrossRef]
24. Harrouz, A.; Colak, I.; Kayisli, K. Control of a small wind turbine system application. In Proceedings of the 2016 IEEE International Conference on Renewable Energy Research and Applications (ICRERA), Birmingham, UK, 20–23 November 2016; pp. 1128–1133.
25. Zhang, X.; Huang, C.; Hao, S.; Chen, F.; Zhai, J. An improved adaptive-torque-gain MPPT control for direct-driven PMSG wind turbines considering wind farm turbulences. *Energies* **2016**, *9*, 977. [CrossRef]
26. Shafiei, A.; Dehkordi, B.M.; Kiyoumarsi, A.; Farhangi, S. A control approach for a small-scale PMSG-based WECS in the whole wind speed range. *IEEE Trans. Power Electron.* **2017**, *32*, 9117–9130. [CrossRef]
27. Oliveira, T.D.; Tofaneli, L.A.; Santos, A.Á.B. Combined effects of pitch angle, rotational speed and site wind distribution in small HAWT performance. *J. Braz. Soc. Mech. Sci. Eng.* **2020**, *42*, 1–18. [CrossRef]
28. Battisti, L.; Benini, E.; Brighenti, A.; Dell'Anna, S.; Castelli, M.R. Small wind turbine effectiveness in the urban environment. *Renew. Energy* **2018**, *129*, 102–113. [CrossRef]
29. Jeong, H.G.; Seung, R.H.; Lee, K.B. An improved maximum power point tracking method for wind power systems. *Energies* **2012**, *5*, 1339–1354. [CrossRef]
30. Zhu, Y.; Cheng, M.; Hua, W.; Wang, W. A novel maximum power point tracking control for permanent magnet direct drive wind energy conversion systems. *Energies* **2012**, *5*, 1398–1412. [CrossRef]
31. Chen, J.H.; Hung, W. Blade fault diagnosis in small wind power systems using mppt with optimized control parameters. *Energies* **2015**, *8*, 9191–9210. [CrossRef]
32. Syahputra, R.; Soesanti, I. Performance Improvement for Small-Scale Wind Turbine System Based on Maximum Power Point Tracking Control. *Energies* **2019**, *12*, 3938. [CrossRef]
33. Aubrée, R.; Auger, F.; Macé, M.; Loron, L. Design of an efficient small wind-energy conversion system with an adaptive sensorless MPPT strategy. *Renew. Energy* **2016**, *86*, 280–291. [CrossRef]
34. Syskakis, T.; Ordonez, M. MPPT for Small Wind Turbines: Zero-Oscillation Sensorless Strategy. In Proceedings of the 2019 IEEE 10th International Symposium on Power Electronics for Distributed Generation Systems (PEDG), Xi'an, China, 3–6 June 2019; pp. 1060–1065.
35. Lopez-Flores, D.R.; Duran-Gomez, J.L.; Chacon-Murguia, M.I. A Mechanical Sensorless MPPT Algorithm for a Wind Energy Conversion System based on a Modular Multilayer Perceptron and a Processor-in-the-Loop Approach. *Electr. Power Syst. Res.* **2020**, *186*, 106409. [CrossRef]
36. Thongam, J.S.; Ouhrouche, M. MPPT control methods in wind energy conversion systems. In *Fundamental and Advanced Topics in Wind Power*; InTech: Vienna, Austria, 2011; pp. 339–360.
37. Martinez, J. Modelling and control of wind turbines. In *Department of Chemical Engineering and Chemical Technology*; Imperial College London: London, UK, 2007.

38. Urtasun, A.; Sanchis, P.; San Martín, I.; López, J.; Marroyo, L. Modeling of small wind turbines based on PMSG with diode bridge for sensorless maximum power tracking. *Renew. Energy* **2013**, *55*, 138–149. [CrossRef]
39. Kot, R.; Rolak, M.; Malinowski, M. Comparison of maximum peak power tracking algorithms for a small wind turbine. *Math. Comput. Simul.* **2013**, *91*, 29–40. [CrossRef]
40. Muhsen, H.; Al-Kouz, W.; Khan, W. Small Wind Turbine Blade Design and Optimization. *Symmetry* **2020**, *12*, 18. [CrossRef]
41. Qi, Z.; Lin, E. Integrated power control for small wind power system. *J. Power Sources* **2012**, *217*, 322–328. [CrossRef]
42. Doll, C.N.; Pachauri, S. Estimating rural populations without access to electricity in developing countries through night-time light satellite imagery. *Energy Policy* **2010**, *38*, 5661–5670. [CrossRef]
43. Raturi, A.K. *Renewables 2016 Global Status Report*; REN21 Secretariat: Paris, France, 2016.
44. Zhang, S.; Qi, J. Small wind power in China: Current status and future potentials. *Renew. Sustain. Energy Rev.* **2011**, *15*, 2457–2460. [CrossRef]
45. Rehman, S.; Sahin, A.Z. Wind power utilization for water pumping using small wind turbines in Saudi Arabia: A techno-economical review. *Renew. Sustain. Energy Rev.* **2012**, *16*, 4470–4478. [CrossRef]
46. Park, J.H.; Chung, M.H.; Park, J.C. Development of a small wind power system with an integrated exhaust air duct in high-rise residential buildings. *Energy Build.* **2016**, *122*, 202–210. [CrossRef]
47. Simic, Z.; Havelka, J.G.; Vrhovcak, M.B. Small wind turbines—A unique segment of the wind power market. *Renew. Energy* **2013**, *50*, 1027–1036. [CrossRef]
48. Parag, Y.; Sovacool, B.K. Electricity market design for the prosumer era. *Nat. Energy* **2016**, *1*, 1–6. [CrossRef]
49. Kortabarria, I.; Andreu, J.; de Alegría, I.M.; Jiménez, J.; Gárate, J.I.; Robles, E. A novel adaptative maximum power point tracking algorithm for small wind turbines. *Renew. Energy* **2014**, *63*, 785–796. [CrossRef]
50. Emejeamara, F.; Tomlin, A.; Millward-Hopkins, J. Urban wind: Characterisation of useful gust and energy capture. *Renew. Energy* **2015**, *81*, 162–172. [CrossRef]
51. Britter, R.; Hanna, S. Flow and dispersion in urban areas. *Annu. Rev. Fluid Mech.* **2003**, *35*, 469–496. [CrossRef]
52. Kumar, A.P.; Parimi, A.M.; Rao, K.U. Investigation of small PMSG based wind turbine for variable wind speed. In Proceedings of the 2015 International Conference on Recent Developments in Control, Automation and Power Engineering (RDCAPE), Noida, India, 12–13 March 2015; pp. 107–112.
53. Askarov, A.; Andreev, M.; Ruban, N. Impact assessment of full-converter wind turbine generators integration on transients in power systems. In *AIP Conference Proceedings*; AIP Publishing LLC: Melville, NY, USA, 2020; Volume 2212, p. 020005.
54. Pillay, P.; Krishnan, R. Modeling of permanent magnet motor drives. *IEEE Trans. Ind. Electron.* **1988**, *35*, 537–541. [CrossRef]
55. Fitzgerald, A.E.; Kingsley, C.; Umans, S.D.; James, B. *Electric Machinery*; McGraw-Hill: New York, NY, USA, 2003; Volume 5.
56. Shariatpanah, H.; Fadaeinedjad, R.; Rashidinejad, M. A new model for PMSG-based wind turbine with yaw control. *IEEE Trans. Energy Convers.* **2013**, *28*, 929–937. [CrossRef]
57. Ata, R.; Koçyigit, Y. An adaptive neuro-fuzzy inference system approach for prediction of tip speed ratio in wind turbines. *Expert Syst. Appl.* **2010**, *37*, 5454–5460. [CrossRef]
58. Anelion SW 3.5 GT. Available online: https://www.wind-turbine-models.com/turbines/950-anelion-sw-3.5-gt (accessed on 25 August 2020).
59. Samar, A.; Saedin, P.; Tajudin, A.I.; Adni, N. The implementation of Field Oriented Control for PMSM drive based on TMS320F2808 DSP controller. In Proceedings of the 2012 IEEE International Conference on Control System, Computing and Engineering, Penang, Malaysia, 23–25 November 2012; pp. 612–616.
60. Salles, M.B.; Hameyer, K.; Cardoso, J.R.; Grilo, A.; Rahmann, C. Crowbar system in doubly fed induction wind generators. *Energies* **2010**, *3*, 738–753. [CrossRef]
61. Kim, Y.S.; Chung, I.Y.; Moon, S.I. Tuning of the PI controller parameters of a PMSG wind turbine to improve control performance under various wind speeds. *Energies* **2015**, *8*, 1406–1425. [CrossRef]

62. Widanagama Arachchige, L.N.; Rajapakse, A.D.; Muthumuni, D. Implementation, comparison and application of an average simulation model of a wind turbine driven doubly fed induction generator. *Energies* **2017**, *10*, 1726. [CrossRef]
63. Kim, C.; Gui, Y.; Zhao, H.; Kim, W. Coordinated LVRT Control for a Permanent Magnet Synchronous Generator Wind Turbine with Energy Storage System. *Appl. Sci.* **2020**, *10*, 3085. [CrossRef]
64. Das, K.; Hansen, A.D.; Sørensen, P.E. Understanding IEC standard wind turbine models using SimPowerSystems. *Wind Eng.* **2016**, *40*, 212–227. [CrossRef]